



Prostaglandins D₂ and E₂ have opposite effects on alveolar macrophages infected with *Histoplasma capsulatum*^S

Priscilla A. T. Pereira,* Patrícia A. Assis,* Morgana K. B. Prado,* Simone G. Ramos,[†] David M. Aronoff,[§] Francisco W. G. de Paula-Silva,* Carlos A. Sorgi,* and Lúcia H. Faccioli^{1,*}

Departamento de Análises Clínicas,* Toxicológicas e Bromatológicas, Faculdade de Ciências Farmacêuticas de Ribeirão Preto, and Departamento de Patologia,[†] Faculdade de Medicina de Ribeirão Preto, Universidade de São Paulo, 14040-903 Ribeirão Preto, São Paulo, Brazil; and Department of Medicine,[§] Division of Infectious Diseases, Vanderbilt University Medical Center, Nashville, TN 37232

ORCID IDs: 0000-0003-4587-6121 (D.M.A.); 0000-0001-8559-532X (F.W.G.P.); 0000-0001-7528-9935 (C.A.S.); 0000-0002-4999-8305 (L.H.F)

Abstract Prostaglandin E₂ (PGE₂) suppresses macrophage effector mechanisms; however, little is known about the function of PGD₂ in infected alveolar macrophages (AMs). Using serum-opsonized *Histoplasma capsulatum* (Ops-*H. capsulatum*) in vitro, we demonstrated that AMs produced PGE₂ and PGD₂ in a time-dependent manner, with PGE₂ levels exceeding those of PGD₂ by 48 h postinfection. Comparison of the effects of both exogenous PGs on AMs revealed that PGD₂ increased phagocytosis and killing through the chemoattractant receptor-homologous molecule expressed on Th2 lymphocytes receptor, whereas PGE₂ had opposite effects, through E prostanoid (EP) receptor 2 (EP2)/EP4-dependent mechanisms. Moreover, PGD₂ inhibited phospholipase C- γ (PLC- γ) phosphorylation, reduced IL-10 production, and increased leukotriene B₄ receptor expression. In contrast, exogenous PGE₂ treatment reduced PLC- γ phosphorylation, p38 and nuclear factor κ B activation, TNF- α , H₂O₂, and leukotriene B₄, but increased IL-1 β production. Using specific compounds to inhibit the synthesis of each PG in vitro and in vivo, we found that endogenous PGD₂ contributed to fungicidal mechanisms and controlled inflammation, whereas endogenous PGE₂ decreased phagocytosis and killing of the fungus and induced inflammation. **Figure 1** These findings demonstrate that, although PGD₂ acts as an immunostimulatory mediator to control *H. capsulatum* infection, PGE₂ has immunosuppressive effects, and the balance between these two PGs may limit collateral immune damage at the expense of microbial containment.—Pereira, P.A.T., P. A. Assis, M. K. B. Prado, S. G. Ramos, D. M. Aronoff, F. W. G. de Paula-Silva, C. A. Sorgi, and L. H. Faccioli. **Prostaglandins D₂ and E₂ have opposite effects on alveolar**

macrophages infected with *Histoplasma capsulatum*. *J. Lipid Res.* 2018. 59: 195–206.

Supplementary key words histoplasmosis • phagocytosis • fungicidal activity

Histoplasmosis is a fungal disease caused by *Histoplasma capsulatum*, mainly affecting the respiratory tract (1). The incidence of histoplasmosis has increased worldwide, which is mostly associated with immunodeficiency, such as HIV (2–4). In the lung, the immune response begins after the uptake of the fungus by alveolar macrophages (AMs) and dendritic cells. AMs have a special importance in lung defense, where they are responsible for protecting the alveolar epithelium by clearing microorganisms by phagocytosis and intracellular killing (5). These innate immune sentinel cells are among the first and most essential participants in the successful elimination of the fungus. Furthermore, AM-derived cytokines and lipid mediators induce neutrophil and mononuclear cell recruitment (5) and activation of adaptive immune responses (6, 7), and regulate phagocytosis and antimicrobial activities of phagocytic cells (5, 7, 8).

In particular, the synthesis and signaling of lipid mediators known as leukotrienes (LTs) and prostaglandins (PGs)

Abbreviations: AM, alveolar macrophage; BLT1, leukotriene B₄ receptor; CFU, colony-forming unit; COX, cyclooxygenase; DPI1, D prostanoid receptor 1; DP2, chemoattractant receptor-homologous molecule expressed on Th2 lymphocytes; EP, E prostanoid; IS, immune serum; JNK1/2, c-Jun N-terminal kinase 1/2; LT, leukotriene; MFI, mean of relative fluorescence units; MOI, multiplicity of infection; NF- κ B, nuclear factor κ B; ops-*H. capsulatum*, opsonized *Histoplasma capsulatum*; PG, prostaglandin; PKA, protein kinase A; PLC- γ , phospholipase C- γ .

¹To whom correspondence should be addressed.

e-mail: faccioli@fcfrp.usp.br

S The online version of this article (available at <http://www.jlr.org>) contains a supplement.

This study was supported by Fundação de Amparo à Pesquisa do Estado de São Paulo Grants Process 2009/07169-5 and 2014/07125-6; and the Conselho Nacional de Desenvolvimento Científico e Tecnológico. The funders had no role in the study design, data collection and analysis, decision to publish, or preparation of the paper. The authors declare that there are no conflicts of interest.

Manuscript received 24 July 2017 and in revised form 5 December 2017.

Published, JLR Papers in Press, December 7, 2017

DOI <https://doi.org/10.1194/jlr.M078162>

are increased during histoplasmosis and further regulate host defense (8, 9). Biosynthesis of PGs is coordinated by two distinct cyclooxygenase (COX) isoforms, the constitutive COX-1 and the inducible COX-2, which convert arachidonic acid (AA) to the unstable intermediate compound PGH₂. Then, terminal synthase enzymes, including PGD and PGE synthases, generate PGD₂ and PGE₂, respectively, at sites of inflammation, resulting in either proinflammatory or anti-inflammatory effects, depending on the nature of the stimulus (10, 11). Recently, we demonstrated that, during lethal *H. capsulatum* infection, pharmacological inhibition of COX-2 by the compound celecoxib increased mouse survival and the phagocytic capacity of AMs, suggesting a contribution of PGs to pathogenesis of this infection (8). Additionally, during bacterial and other fungal infections, PGE₂ and PGD₂ production is enhanced in the lung (8, 12). However, the specific roles of PGD₂ and PGE₂ during infections, especially in histoplasmosis, remain incompletely defined.

Over time, PGE₂ has emerged as a potent endogenous modulator of innate immunity and macrophage effector functions (10, 13). Generally, PGE₂ promotes endothelial cell-mediated vasodilatation and recruitment of circulating leukocytes during inflammation to areas of infection, through mechanisms activated by PGE₂ binding to E prostanoïd (EP) receptors (EP1–4) coupled to G proteins present in the cell membrane (13). On the other hand, PGE₂ inhibits macrophage effector mechanisms, such as phagocytosis, through EP2 receptor and bacterial killing through EP2–4 receptors, both coupled to G α s proteins, leading to activation of adenylate cyclase, which increases cyclic adenosine monophosphate (cAMP) concentrations (14–16) and IL-1 β production (16). PGD₂, in turn, binds to the D prostanoïd receptor 1 (DP1) and to the “chemoattractant receptor-homologous molecule expressed on Th2 lymphocytes” receptor (DP2 or CRTH2) (17). PGD₂ binds to DP1, a transmembrane receptor coupled to the G-protein subunit G α s. This prostanoïd also induces elevation of cAMP, resulting in the inhibition of effector mechanisms of macrophages and other cells (18–20). However, when PGD₂ binds to DP2, a G α i protein subunit coupled receptor, it reduces cAMP concentrations (21). Consequently, the potentially contrasting immunoregulatory roles of PGD₂ and PGE₂ require further investigation, which is the focus of the present research.

Mammalian cells communicate with each other by exchanging signals that bind specifically to surface or intracellular receptors, followed by a cascade of events that amplify and transduce the incoming signal and eventually elicit a cellular response. The cAMP-dependent protein kinase A (PKA), mitogen-activated protein kinase (MAPK), and nuclear factor κ B (NF- κ B) cascades modulate common processes in the cell, and multiple levels of cross-talk between these signaling pathways have been described (22, 23). Because activation of PG receptors/cAMP axes is important to regulate macrophage effector functions (14, 15), the putative role of PGD₂ and PGE₂ in cell signaling activation and inflammatory mediator synthesis deserves detailed examination.

Despite the fact that PGE₂ has been shown to inhibit phagocytosis and killing of pathogens by macrophages (14, 15), the role of PGD₂ in modulating AM effector functions is not known. In the present study, we determined the contribution of endogenous and exogenous PGD₂ and PGE₂ on AM effector functions after immune serum (IS)-opsonized *H. capsulatum* (*Ops-H. capsulatum*) infection. Using rat AMs, we found that endogenous and exogenous PGD₂ and PGE₂ actions result in divergent effects on phagocytosis and fungicidal activities of these cells. Treatment of *Ops-H. capsulatum*-infected AMs with exogenous PGD₂ increased phagocytosis and killing through the DP2 receptor; it also inhibited phosphorylation of phospholipase C- γ (PLC- γ) without affecting c-Jun N-terminal kinase 1/2 (JNK1/2), p38, and NF- κ B. Furthermore, PGD₂ inhibited IL-10 production by infected AMs, while increasing the expression of high-affinity receptors for LTB₄ (BLT1). An opposite effect was observed for PGE₂, which reduced phagocytosis and killing through an EP2/EP4-dependent manner. Additionally, it diminished phosphorylation of PLC- γ , p38, and NF- κ B, while amplifying JNK1/2, and reducing TNF- α , H₂O₂, and LTB₄ production by *Ops-H. capsulatum*-infected AMs. Finally, in vivo experiments demonstrated that inhibition of PGD₂ synthesis increased susceptibility to infection in mice, as well as increased inflammatory cytokine production, while inhibition of PGE₂ synthesis increased resistance against infection and diminished lung tissue damage. Also, endogenous PGD₂ regulated only fungicidal mechanisms, whereas endogenous PGE₂ coordinated phagocytosis and killing of the fungus by AMs. Given the opposite effects of PGD₂ and PGE₂ during AM infection, these lipids might be potential targets to treat fungal lung diseases, particularly histoplasmosis.

MATERIALS AND METHODS

Animals

Pathogen-free male Wistar rats (125–150 g) and male C57BL/6 mice (20–22 g) were obtained from the animal facilities of the Faculdade de Ciências Farmacêuticas de Ribeirão Preto, Universidade de São Paulo. All experiments were approved and conducted in accordance with the guidelines of the Animal Care Committee of the University of São Paulo (Protocols 09.1.375.53.5 and 013.2016-1). The in vitro experiments with *H. capsulatum*-infected AMs and infected animals were performed in level 3 biohazard facilities at Faculdade de Medicina de Ribeirão Preto, Universidade de São Paulo.

Culture of *H. capsulatum*

The *H. capsulatum* clinical isolate was obtained from a patient at the Hospital das Clínicas, Faculdade de Medicina de Ribeirão Preto, Universidade de São Paulo. The mycelia were obtained by culturing fungi at 25°C in Sabouraud dextrose agar tubes (Difco, Detroit, MI), and the live yeast fungus was subcultured at 37°C on glutamine-cysteine-sheep blood (5%) BHI (Detroit, MI) for 15 days. Yeast cells were used when their viability was $\geq 90\%$ according to fluorescein diacetate (Sigma-Aldrich, St. Louis, MO) and ethidium bromide (Sigma-Aldrich) staining (8, 9).

IS and opsonization

Rats were intraperitoneally inoculated with 1 ml containing 10⁸ yeast of *H. capsulatum*, and 10 days later were submitted to a second

inoculation with an equal inoculum. After 7 days, the rats were decapitated, and blood was collected and centrifuged at 1,900 g for 10 min to obtain the IS. IS was heated at 56°C for 1 h to inactivate complement proteins and stored at -80°C (24). For fungus opsonization, 1×10^8 yeast in 1 ml of PBS was incubated with 10% IS for 30 min at 37°C on a rotating platform (7), and the opsonized fungus is referred to as Ops-*H. capsulatum*. Nonopsonized fungi (*H. capsulatum*) incubated only with PBS were used for comparison as described.

AM isolation, cell culture, and treatments

Resident AMs from naïve rats were obtained via ex vivo lung lavage (24) and suspended in incomplete RPMI 1640 at 2×10^6 cells per ml. Cells were allowed to adhere to tissue culture plates for 1 h (37°C, 5% CO₂), followed by two washes with warm incomplete RPMI 1640, resulting in $\pm 99\%$ of adherent cells identified as AMs by staining with Panoptic (Laborclin, Paraná, Brazil). Cells were cultured overnight in complete RPMI 1640 containing 10% FBS and 1% penicillin/streptomycin/amphotericin B (Gibco, Grand Island, NY). The following day, cells were washed twice with warm medium (incomplete RPMI 1640) to remove nonadherent cells. AMs were preincubated with indomethacin (10 μ M) (COX1/2 inhibitor; Sigma-Aldrich), or celecoxib (10 μ M) (COX-2 inhibitor; Celebra®, Pfizer, SP, Brazil), or HQL-79 (1 μ M) (PGD₂ synthase inhibitor); or CAY10526 (1 μ M) (PGE₂ synthase inhibitor); or BWA868c (1 μ M) (DP1 antagonist); or Bay-u3405 (1 μ M) (DP2 antagonist); or AH6809 (1 μ M) (EP2 antagonist); or AH23848 (1 μ M) (EP4 antagonist), preceding fungus infection. The enzyme inhibitors or antagonists were purchased from Cayman Chemical (Ann Arbor, MI), and incubated with AMs for 30 min before infection. When necessary, cells were incubated with PGD₂ or PGE₂ for 2 min (1 μ M) (Cayman Chemical), before in vitro infection. Receptor antagonist and concentrations used were previously determined by our group (16, 25) or investigated in the literature (14, 15, 26, 27). Incomplete RPMI 1640 containing the same concentrations of DMSO and/or alcohol used to dissolve the compounds was used as control and identified as vehicle. Cells treated with compounds or vehicle were used for phagocytic and fungicidal assays.

Fluorometric phagocytosis assay with FITC-labeled *H. capsulatum*

A fluorometric phagocytosis assay was performed to test the capacity of AMs to phagocytize FITC-labeled *H. capsulatum* (or Ops-*H. capsulatum*) as published previously (7). Briefly, yeast cells were labeled with FITC (Amresco, OH) for 1 h at 37°C (7). FITC-labeled Ops-*H. capsulatum* or FITC-labeled *H. capsulatum* was added, and the number of yeast cells to be used by AMs was determined through multiplicity of infection (MOI) starting from 1:1; 1:5, or 1:10, respectively. The AMs were pretreated or not with the compounds as described above before the fungus was added and then incubated in the dark (37°C, 5% CO₂). After 2 h, free yeast cells were removed by washing with warm sterile PBS, and the residual extracellular FITC was quenched with Trypan blue (250 mg/ml; Gibco) for 1 min. Fluorescence was determined by using a micro plate reader (485 nm excitation/535 nm emission, SPECTRA-Max, Molecular Devices, Sunnyvale, CA). Phagocytosis was determined by the mean of relative fluorescence units (MFI) emitted from intracellular fungi.

Fungicidal activity assay

AMs were pretreated with IFN- γ (50 ng/ml) overnight to improve their effector mechanism as described by Peck (28), and submitted or not to the above treatments. Next, cells were incubated with *H. capsulatum* (opsonized or not) at MOI 1:10, and after 2 h, cells were washed twice with warm sterile PBS to remove

the extracellular yeasts. Following another 48 h of incubation, the supernatants were collected and kept at -80°C until they were used for measurements, as described. Afterward, the cells were lysed by adding 200 μ l of 0.05% saponin, and an aliquot was plated on BHI agar-blood (29). After 21 days of culture at 37°C, the colony-forming units (CFU) were counted and the fungicidal activity was calculated according to the formula: $[100 - (100 \times \text{CFU experimental}) / \text{CFU control}]$.

Quantitation of cytokines

AMs treated or not with the above compounds were incubated with Ops-*H. capsulatum*, and after 48 h the cell culture supernatants or lung homogenate of *H. capsulatum*-infected mice were obtained to measure TNF- α , IL-1 β , and IL-10, by using commercially available ELISA kits (R&D Systems, Minneapolis, MN). For each sample, the cytokine concentrations were obtained from a standard curve established with the appropriate recombinant cytokine. The sensitivities were >10 pg/ml.

Hydrogen peroxide production

The release of H₂O₂ from AMs was determined by phenol red oxidation, as described previously (30), in supernatant from cells pretreated or not with PGD₂ or PGE₂, and incubated with Ops-*H. capsulatum* (MOI 1:10). After 48 h of incubation, the supernatants were replaced by supplemented assay medium (RPMI 1640-containing peroxidase and phenol red) and incubated for 2 h. Then, stop solution (NaOH 1N) was added, and optical density (OD) was determined at 620 nm.

Flow-cytometry analysis of BLT1 expression in AMs

The expression of BLT1 was determined by using the flow-cytometry immune staining protocol with antibodies conjugated with fluorochromes (BD Biosciences, Franklin Lakes, NJ). The AMs (2×10^5 cells) were pretreated with the compounds described above before the fungus was added (2×10^4 cells) and incubated at 37°C, 5% CO₂. After 2 h, the supernatant was removed, and the cells were washed with 300 μ l of PBS containing 2% FBS (Gibco). Cells were then suspended in polystyrene tubes and centrifuged at 400 g for 5 min. Cells were suspended in Fc block (200 μ l), containing anti-CD16/CD32 antibodies at dilution 1:100 and incubated for 30 min at 4°C. Subsequently, the antibody against BLT1 was added to the AMs. After 40 min, cells were washed twice, and then fixed with PBS containing 1% (wt/vol) paraformaldehyde. A total of 20,000 events was acquired for each tube (FACSCanto™; Becton Dickinson), using the FACSDiva software.

Measurements of PGE₂, PGD₂, and LTB₄

Eicosanoids were purified from the supernatant of AMs cultures or lung homogenate (Mixer Homogenizer, IKA, Wilmington, NC) by using Sep-Pak C18 cartridges according to the manufacturer's instructions (Waters Corp., Milford, MA). Quantifications of PGE₂ and LTB₄ (Enzo Life Science, Farmingdale, NY) and PGD₂ (Cayman Chemical) were performed by using specific enzyme immunoassay kits according to manufacturers' instructions, and the results were expressed in picograms per milliliter, or, after the data were transformed, as percentages, and infected AM was set as 100%.

Phosphoprotein detection by cytometric bead array

Samples of AMs were prepared as previously described (31). After infection and treatments, cells were washed with ice-cold PBS and then lysed with buffer containing protease and phosphatase inhibitors according to the manufacturer's protocol for adherent cells (Becton Dickinson, Heidelberg, Germany). The cell lysates were moved to Eppendorf tubes and immediately placed in

a boiling water bath for 5 min. The total protein concentration was adjusted to 1 µg/µl, and the cell lysates were stored at -80°C until measurement of kinase phosphorylation. The total protein content of the lysates was determined by using the Bradford method (Sigma-Aldrich). Quantitative determination of phospho-JNK1/2 (T183/Y185), phospho-p38 (T180/Y182), and phospho-PLC-γ (Y783) was performed by using antibodies from the multiplex Flex Set Cytometric Bead Array (Becton Dickinson). Flow-cytometric analysis was performed using FACSCanto™, and FACSDiva was used for data acquisition and analysis (Becton Dickinson). A total of 900 events was acquired.

RAW-Blue™ cells experiment

To analyze the influence of PGE₂ and PGD₂ on NF-κB activation induced by the fungus, we used RAW-Blue™ cells (InvivoGen). RAW-Blue™ is a cell line of macrophages that stably express the SEAP gene (secreted embryonic alkaline phosphatase), which is induced by NF-κB/AP-1 transcription factors and confers resistance to Zeocin™. These cells were grown in DMEM supplemented with 10% FBS, Normocin™ (50 µg/ml), and Zeocin™ (25 µg/ml). The cells were seeded in 96-well microculture plates at a density of 2 × 10⁵ cells per well in DMEM supplemented with Normocin™ (50 mg/ml) and cultured at 37°C in a humidified 5% CO₂ atmosphere for 18 h. After this period, the cells were stimulated with PGD₂ or PGE₂ for 2 min and then incubated with *Ops-H. capsulatum* (2 × 10⁴ yeast per well) for 24 h. After this period, the medium was collected, and samples of 50 µl were mixed in 96-well plates at 37°C for 2 h, with 150 µl of QUANTI-Blue™ (InvivoGen), which is a SEAP detection medium. The OD was then measured at 650 nm by using an ELISA reader (µQuant, Biotek Instruments Inc., Winooski, VT).

Infection and in vivo pharmacological treatments

Mice were anesthetized with ketamine and xylazine (10 and 20 mg/kg, respectively) and restrained on a small board. A 30-gauge needle attached to a tuberculin syringe was inserted into the trachea, and a lethal inoculum of *H. capsulatum* in PBS (1 × 10⁶ yeast/100 µl per mouse) was intratracheally dispensed into the lungs. Infected mice were treated by gavage with inhibitor of PGD₂ synthase (HQL-79, Cayman Chemical; 3 mg/kg/0.5 ml of water, dose chosen based on dose-response experiments ranging from 0.3 to 3 mg/kg) (32), or inhibitor of PGE₂ synthase (CAY10526, Cayman Chemical; 5 mg/kg/0.5 ml of water) (33) or water (0.5 ml), 1 h before infection and daily for 30–40 days. As a control, mice were injected with PBS and treated daily with water.

Histology

At 7 days postinfection, the lungs were removed and immediately fixed in 10% formalin for conventional histological examination. The specimens were processed, embedded in paraffin, and cut into 5-µm sections. The sections were stained with hematoxylin and eosin (H&E) and analyzed in a blinded fashion at 100× magnification. ImageJ software (NIH, Bethesda, MD) was used to calculate the lung area damage in five random photomicrograph sections per slide, which was represented by percent lung area covered by infiltrating cells calculated for each mouse by dividing the sum of damage areas in these sections by the total area of the lung examined.

Determination of CFU

After 7 days of infection, the lungs were recovered to determine the fungal burden. *H. capsulatum* yeasts from the lung were examined as previously described (9). Two hundred microliter samples from each cell suspension were collected, and a 10-fold

dilution was plated into BHI agar-blood. After incubation at 37°C for 21 days, the *H. capsulatum* CFU was counted and expressed as CFU/g lung (log 10).

Statistical analysis

Statistical analysis was performed by using GraphPad Prism 5.0 (GraphPad Software, La Jolla, CA). Data are expressed as mean ± standard error of the mean (SEM). All experiments were conducted in triplicate unless otherwise noted, and repeated at least twice. Comparisons were performed by using ANOVA followed by Tukey's multiple comparison test as described. In all comparisons, a significance level of *P* < 0.05 was considered to be significant. Differences in survival were analyzed by using the log-rank test. Significance level was set at 5%.

RESULTS

In vitro AMs phagocytized *Ops-H. capsulatum* more efficiently and released PGE₂ and PGD₂ differently

The usual immune response to *H. capsulatum* begins in the lung with the uptake of the fungus by resident AMs that are essential cells for clearing microorganisms by phagocytosis and intracellular killing (29). In addition, it has been demonstrated that *H. capsulatum* induces a humoral immune response and leads to production of circulating immune complexes (34). Since a humoral response is enhanced during the course of infection (34), it may be relevant in the setting of reinfection, particularly in endemic areas. Therefore, we first investigated whether resident AMs produce PGD₂ and PGE₂ after in vitro infection with nonopsonized (*H. capsulatum*) or with specific IS-opsonized *H. capsulatum* (*Ops-H. capsulatum*). As expected, after 2 h, *Ops-H. capsulatum* was more efficiently phagocytized than the nonopsonized fungus (Fig. 1A). The phagocytosis induced PGE₂ production by AMs 2 and 48 h following infection, whereas PGD₂ production was increased only at 48 h (Fig. 1B, C). The nonopsonized fungus induced lower amounts of PGs in comparison to the opsonized fungus. Based on these data, *Ops-H. capsulatum* was selected for the next experiments to assess the effects of PGD₂ and PGE₂ on AM effector functions.

Inhibition of COX-1 and COX-2 increased phagocytosis and fungicidal activity of AMs and diminished PGD₂ and PGE₂ production

We next evaluated the extent to which endogenous PGs are required during FcR-mediated phagocytosis and killing of *H. capsulatum* by AMs. AMs were pretreated with indomethacin (10 µM), a dual COX-1/COX-2 inhibitor, or celecoxib (10 µM), a selective COX-2 inhibitor, and 30 min later were infected with IgG-*H. capsulatum*. Both inhibitors increased phagocytosis of *Ops-H. capsulatum* by AMs (Fig. 2A). Next, we evaluated the role of PGs in the fungicidal activity of AMs after 48 h of incubation with *Ops-H. capsulatum*. Nonspecific inhibition of COX enzymes or the specific inhibition of COX-2 augmented clearance of IgG opsonized fungi by AMs (Fig. 2B). As expected, both COX inhibitors suppressed the production of PGD₂ and PGE₂

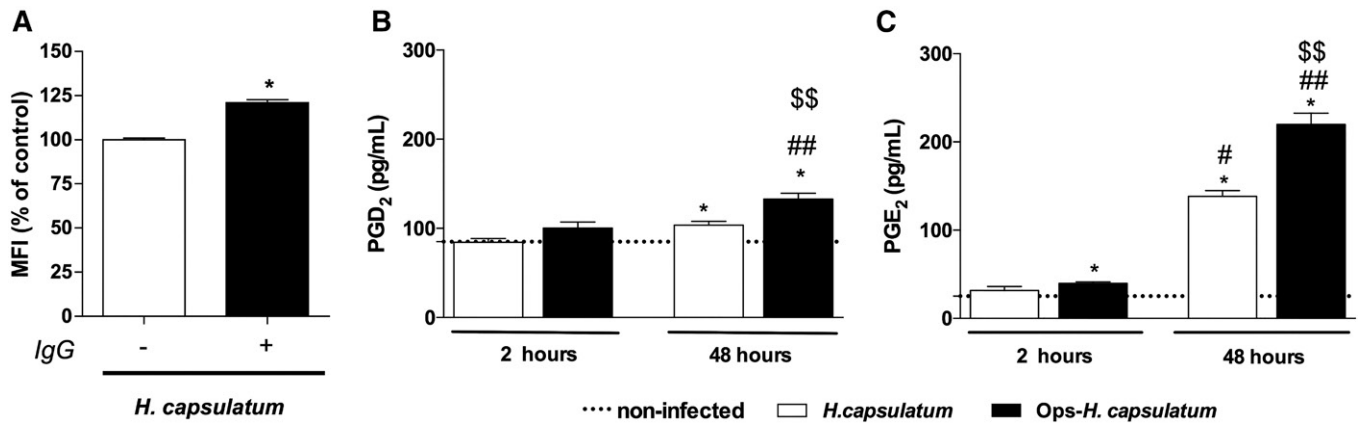


Fig. 1. *Ops-H. capsulatum* are more efficiently phagocytized by AMs and induced higher amounts of PGE₂ and PGD₂ than did *H. capsulatum*. **A:** AMs were incubated with *H. capsulatum* or *Ops-H. capsulatum* labeled with FITC (MOI 1:10), and phagocytosis was assessed 2 h later. Data are expressed as average of fluorescence intensity (MFI) from internalized yeast (n = 6). To determine PGD₂ (**B**) and PGE₂ (**C**) production, AMs were incubated with *H. capsulatum* or *Ops-H. capsulatum* (MOI 1:10) during 2 and 48 h, and the supernatants were collected for PG quantification by immunoassays as described in Materials and Methods (n = 3). * *P* < 0.05 [*H. capsulatum* vs. *Ops-H. capsulatum* (**A**); noninfected AMs vs. AMs + *H. capsulatum* or vs *Ops-H. capsulatum* (**B, C**)]; # *P* < 0.05 (48 h AMs + *H. capsulatum* vs. 2 h *H. capsulatum*); ## *P* < 0.05 (48 h AMs + *Ops-H. capsulatum* vs. 2 h *Ops-H. capsulatum*); \$\$ *P* < 0.05 (48 h AMs + *H. capsulatum* vs. 48 h *Ops-H. capsulatum*). One-way ANOVA and Tukey's multiple comparison tests were used. Data are representative of two independent experiments (±SEM).

(Fig. 2C, D). Our data demonstrate that inhibition of COX-1- or COX-2-mediated PG synthesis during fungal infection increased the phagocytic and fungicidal activity of AMs against *Ops-H. capsulatum*.

PGD₂ and PGE₂ have opposite effects on phagocytosis and fungicidal activity of AMs infected with *Ops-H. capsulatum*

It has been demonstrated that PGE₂ inhibits bacterial phagocytosis and killing by AMs (14, 15). Because we detected that both PGD₂ and PGE₂ are produced by AMs infected with *H. capsulatum* (Fig. 1), we subsequently investigated the biological effect of each PG in regulating phagocytosis and killing by AMs. First, we

showed that the inhibition of endogenous PGD₂ synthesis by HQL-79 at 1 μM (Fig. 3A) (and at other concentrations of 0.1 and 10 μM; data not shown) did not modify phagocytosis of *Ops-H. capsulatum* by AMs. In contrast, inhibition of endogenous PGE₂ by CAY10526 at 2 μM increased phagocytosis (Fig. 3B) (and at other concentrations of 0.2 and 20 μM; data not shown). Next, we evaluated the effects of exogenous administration of each PG on phagocytosis. The addition of exogenous PGD₂ (1 μM) increased (Fig. 3A), whereas exogenous PGE₂ (1 μM) inhibited phagocytosis (Fig. 3B) of IgG-*H. capsulatum*. Inhibition of endogenous PGD₂ or PGE₂ did not distinctively alter the effects of the exogenous mediators (Fig. 3A, B).

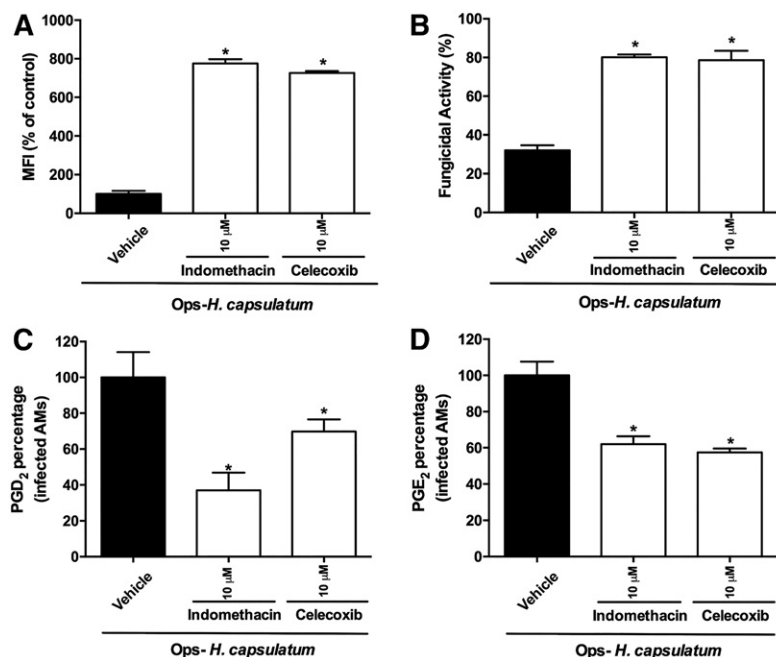


Fig. 2. Inhibition of COX-1 and COX-2 decreased PGD₂ and PGE₂ and augmented phagocytosis and fungicidal activity of AMs. **A:** AMs were pretreated or not with indomethacin (10 μM) or celecoxib (10 μM) for 30 min prior to addition of *Ops-H. capsulatum* labeled with FITC (MOI 1:10). Phagocytosis was assessed 2 h later. Data are expressed as average of fluorescence intensity (MFI) from internalized yeast (n = 6). **B:** AMs were incubated with *Ops-H. capsulatum* at MOI 1:10 for 2 h to allow yeast internalization, and, after 48 h, AMs were lysed, and live yeast was determined by CFU number. Fungicidal activity was expressed as a percentage from total internalized yeast (100%) (n = 4). Measurement of PGD₂ (**C**) and PGE₂ (**D**) by immunoassays is described in Materials and Methods. The supernatants were collected 2 h after indomethacin or celecoxib treatment and fungal infection (n = 4). Production of PGD₂ and PGE₂ was expressed as a percentage, and infected and vehicle-incubated cells were set as 100% (AMs + *Ops-H. capsulatum*). * *P* < 0.05 [AMs + *Ops-H. capsulatum* (in vehicle) vs. other groups]. One-way ANOVA–Tukey's multiple comparison tests were used. Data are representative of two independent experiments (±SEM).

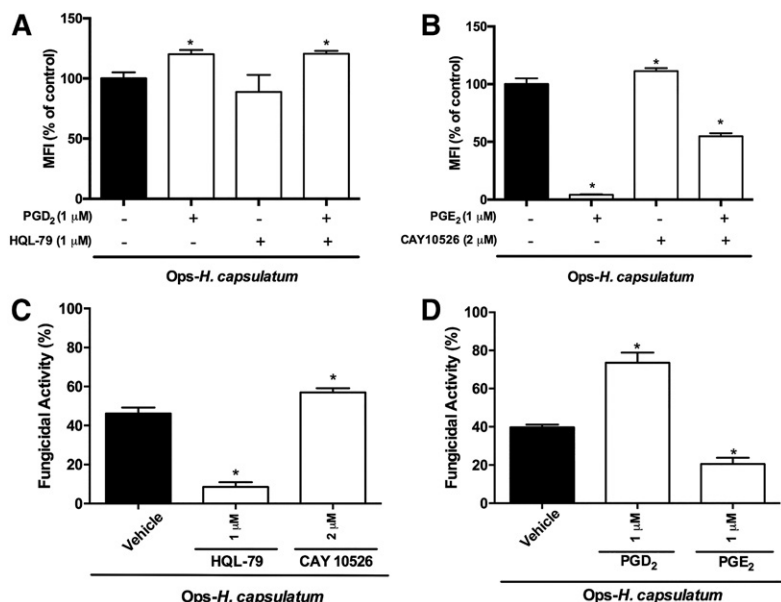


Fig. 3. PGD₂ and PGE₂ have opposite effects on phagocytosis and fungicidal activity of AMs. The effects of pretreating AMs with a specific inhibitor of PGD synthase (HQL-79) or PGE synthase (CAY10526), or soluble PGD₂ or PGE₂ on phagocytosis and fungicidal activity were assessed. AMs were pretreated with HQL-79 (1 μM) or/and PGD₂ (1 μM) (A) or CAY10526 (2 μM) or/and PGE₂ (1 μM) (B), respectively, 30 and 2 min before the addition of *Ops-H. capsulatum* (MOI 1:10) labeled with FITC. Phagocytosis was assessed 2 h later, and data are expressed as average of fluorescence intensity (MFI) from internalized yeast (n = 6). The fungicidal activity was also evaluated following treatment with HQL-79 or CAY10526 (C) or with PGD₂ or PGE₂ (D). After 48 h, AMs were lysed, and CFU number determined live yeast. Fungicidal activity was expressed as a percentage from total internalized yeast by AMs incubated with vehicle (100%) (n = 4). * *P* < 0.05 [AMs + *Ops-H. capsulatum* (in vehicle) vs. other groups]. One-way ANOVA and Tukey's multiple comparison tests were used. Data are representative of two independent experiments (±SEM).

Interestingly, we also found that, after 48 h, inhibition of PGD synthase impaired the killing of *Ops-H. capsulatum* by AMs, whereas inhibition of PGE synthase increased this process (Fig. 3C). These findings indicate that the inhibition of endogenous PGD₂ exerted no effect on the phagocytic ability of AMs. However, these treatments regulated the fungicidal activity of infected AMs differently. Adding exogenous PGD₂ and PGE₂, we confirmed that PGD₂ increased the killing of IgG-*H. capsulatum*, whereas PGE₂ reduced the ability of AMs to eliminate the fungus (Fig. 3D). Together, these data indicate the opposite effects of PGD₂ and PGE₂ on yeast killing by AMs and demonstrate, for the first time, that phagocytosis can be enhanced only by exogenous PGD₂, which, in vivo, may be released by its own cells and other neighbors.

PGD₂ and PGE₂ receptors differently control phagocytosis and killing of *Ops-H. capsulatum* by AMs

PGD₂ and PGE₂ signaling occurs through specific G-coupled receptors to mediate effector mechanisms in macrophages (14, 35). Therefore, we investigated which receptors are driving the effects of exogenous and endogenous PGD₂ and PGE₂ on phagocytosis and killing of *Ops-H. capsulatum* by AMs. Phagocytosis of *Ops-H. capsulatum* was increased by pretreatment of AMs with PGD₂ alone or PGD₂ in presence of a DP1 receptor antagonist (BWA868c), but was reduced after blocking DP2 receptors by the compound Bay-u3405. When used in combination, DP1/DP2 antagonists did not affect PGD₂-increased phagocytosis. Interestingly, blocking DP1, DP2, or DP1/DP2 in the absence of exogenous PGD₂ did not affect the phagocytosis of the fungus (Fig. 4A). On the other hand, in the presence of exogenous PGE₂, an EP2 antagonist (compound AH6809) did not modify its inhibitory effects, whereas an EP4 antagonist (AH23848 compound) potentiated its inhibitory action. Unexpected simultaneous inhibition of EP2/EP4, in the presence of exogenous PGE₂, almost reversed its inhibitory

action. Nevertheless, when AMs were pretreated with EP1 or EP2 antagonists, in the absence of exogenous PGE₂, significant and similar inhibition of phagocytosis was observed, but simultaneous EP2/EP4 blocking had no effect (Fig. 4B).

When the fungicidal activity of AMs was evaluated in the presence of exogenous PGD₂, and DP2 and DP1/DP2 antagonists, its fungicidal activity was reversed, unlike the DP1 antagonist. However, blocking DP1, DP2, or DP1/DP2 in the absence of exogenous PGD₂ did not affect AM killing activity (Fig. 4C). However, only blocking the EP4 receptor potentiated exogenous PGE₂-induced reduction of fungicidal activity of AMs infected with *Ops-H. capsulatum*. Simultaneous inhibition of EP2/EP4 completely blocked the inhibitory effects of exogenous PGE₂. Similar results were observed by pretreating AMs with EP2 and/or EP4 antagonists in the absence of exogenous PGE₂ (Fig. 4D). Together, these data further demonstrate that PGD₂ increased phagocytosis and fungicidal activity through DP2 receptor activation, and PGE₂-impaired phagocytosis and fungicidal activity are mediated by the cooperation of both receptors EP2 and EP4.

PGD₂ and PGE₂ modified PLC-γ, MAPK, and NF-κB/AP-1 signaling during *Ops-H. capsulatum* infection

In order to identify cell signaling pathways activated or inhibited by PGD₂ and PGE₂ during *Ops-H. capsulatum* AM infection, we investigated the phosphorylation of PLC-γ, JNK1/2, and p38 and the activation of NF-κB. As demonstrated by protein phosphorylation, PLC-γ, JNK1/2, p38, and NF-κB/AP-1 pathways were activated in AMs in response to *Ops-H. capsulatum* infection. Although *Ops-H. capsulatum* infection induced PLC-γ phosphorylation, the addition of exogenous PGD₂ or PGE₂ reduced phospho-PLC-γ after 2 h (Fig. 5A). In infected cells, exclusively, PGE₂ potentiated phosphorylation of JNK1/2 at an earlier time point (Fig. 5B), abrogated phosphorylation of p38

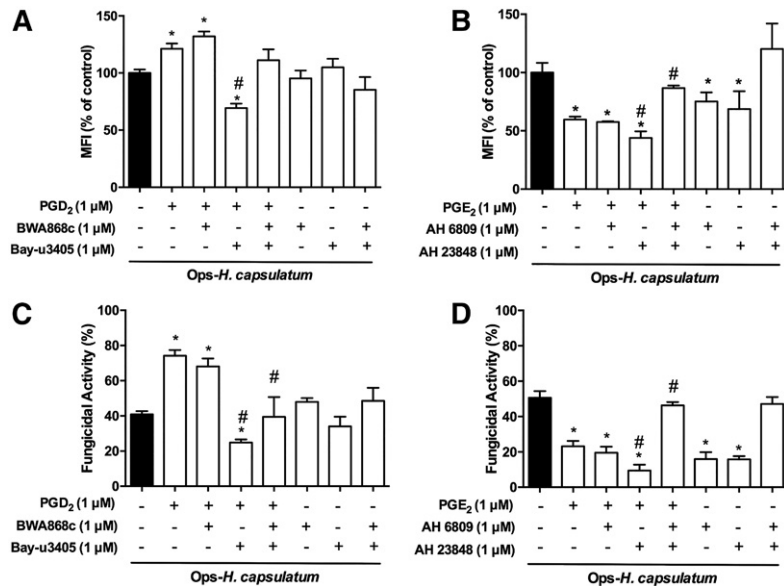


Fig. 4. PGD₂ and PGE₂ receptors antagonists differently impacted phagocytosis and killing of *Ops-H. capsulatum* by AMs. AMs were pretreated or not for 20 min with DPI antagonist (BWA868c; 1 μM) or/and DP2 antagonist (Bay-u3405; 1 μM) before addition of vehicle or PGD₂ (1 μM) for 2 min. Subsequently, the cells were infected with *Ops-H. capsulatum* labeled with FITC (MOI 1:10), and phagocytosis (A) and fungicidal activity (C) were assessed 2 and 48 h later, respectively. In another set of experiments, AMs were pretreated or not with EP2 antagonist (AH 6809; 1 μM) and/or with EP4 antagonist (AH 23848; 1 μM) before the addition of vehicle or PGE₂ (1 μM) for 2 min. Subsequently, the cells were infected with *Ops-H. capsulatum* labeled with FITC (MOI 1:10), and phagocytosis (B) and fungicidal activity (D) were assessed 2 and 48 h later, respectively. Phagocytosis is expressed as average of fluorescence intensity (MFI) from internalized yeast by AMs in vehicle (n = 6). For fungicidal activity, after 48 h, AMs were lysed, and the fungicidal activity was determined as described in Materials and Methods. Fungicidal activity was expressed as a percentage of live yeast recovered (CFU) from cells treated with the antagonists in comparison to total yeast recuperated from AMs incubated with vehicle (100%) (n = 4). * *P* < 0.05 (AMs + *Ops-H. capsulatum* vs. other groups); # *P* < 0.05 (AMs + *Ops-H. capsulatum* PGD₂ or PGE₂ vs. treatments). One-way ANOVA and Tukey's multiple comparison tests were used. Data are representative of four independent experiments (±SEM).

(Fig. 5C), and reduced activation of NF-κB/AP-1. Together, these findings support the hypothesis that PGD₂ and PGE₂ have distinct effects on infected AMs, and that these effects can be mediated through distinct cell-signaling pathways.

Distinct effects of PGD₂ and PGE₂ on production of inflammatory mediators and BLT1 receptor expression by AMs infected with *Ops-H. capsulatum*

In tissues and cells infected by *H. capsulatum*, production of different inflammatory mediators appears to influence the success or failure of the host to control the infection (9, 36–39). Therefore, we investigated the extent to which PGs could modulate TNF-α, IL-1β, IL-10, LTB₄, and H₂O₂ production and BLT1 receptor expression by infected AMs. *Ops-H. capsulatum* infection induced production of all mediators listed above and increased the BLT1 when compared with uninfected cells. Interestingly, TNF-α, IL-10, and H₂O₂ were significantly reduced when AMs were preincubated with PGE₂ (Fig. 6A, C, D), whereas IL-1β was increased (Fig. 6B). In contrast, administration of PGD₂ did not modify TNF-α, IL-1β, and H₂O₂ (Fig. 6A, B, D), but inhibited IL-10 production (Fig. 6C). Specifically, regarding the cross-talk between lipid mediators, we observed that PGE₂ negatively regulated LTB₄ production, unlike PGD₂, which exerted no effect (Fig. 6E). However, only PGD₂ increased the expression of BLT1 induced by the infection (Fig. 6F). These findings reinforce the idea that PGE₂ suppresses proinflammatory mediator production, which in fact might impair fungi elimination by AMs. Alternatively, PGD₂ inhibited the production of IL-10, which represents a negative regulator of phagocytosis and killing,

while simultaneously facilitating LTB₄ beneficial effector functions.

Differential effects of inhibition of PGD₂ and PGE₂ during *H. capsulatum* infection in vivo

Previous experiments in our laboratory showed that PGs are important mediators of the pathogenesis of pulmonary histoplasmosis (8). In this study, we showed that the two PGs had different effects on activating AMs for phagocytosis and killing. To examine the physiological differences between PGD₂ and PGE₂, mice were infected with a lethal *H. capsulatum* inoculum and treated daily with selective PGD₂ or PGE₂ synthesis inhibitors. Infected mice began to die 14 days postinfection; mice treated with the selective inhibitor of PGD synthase HQL-79 showed a higher death rate, whereas mice treated with CAY10526, an inhibitor of microsomal PGE synthase activity, showed increased survival (Fig. 7A). The specificity effect of HQL-79 and CAY10526 was observed 7 days postinfection based on inhibition of PGD₂ and PGE₂ production (Fig. 7B). Also, inhibition of PGD₂ synthesis increased the fungal burden (Fig. 7B). *H. capsulatum*-infected mice treated with CAY10526 decreased TNF-α, IL-1β, and IL-10 production (Fig. 7C). However, HQL-79 treatment significantly increased IL-1β and IL-10 production 7 days after *H. capsulatum* infection (Fig. 7C). The lung inflammation was observed in Fig. 7D, where the inhibition of PGE₂ synthesis decreased inflammatory cell infiltrate and lung damage. These data demonstrate that inhibition of PGD₂ increases the susceptibility of mice to *H. capsulatum* infection, whereas inhibition of PGE₂ increases resistance, but reduces tissue damage.

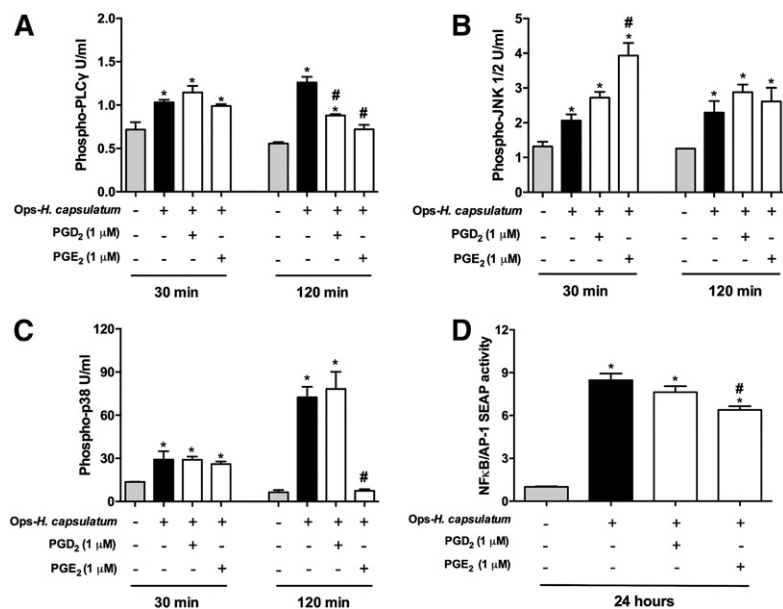


Fig. 5. MAPKs and NF- κ B are involved in PG-induced macrophage activation. Quantification of phosphorylated PLC- γ (A), JNK1/2 (B), and p38 (C) were determined by cytometric bead array and expressed as units per milliliter. Phosphorylation was determined in AMs stimulated with PGD₂ or PGE₂ for 2 min. After the cells were infected with *Ops-H. capsulatum* infection (MOI 1:10) for 30 and 120 min, the cells were analyzed. Nontreated and noninfected cells were used as controls. D: Activation of NF- κ B/AP-1 was measured in RAW-BlueTM cells incubated with either PGD₂ or PGE₂ for 2 min, before addition of *Ops-H. capsulatum* (MOI 1:10) for 24 h. * $P < 0.05$ (uninfected AMs vs. other groups); # $P < 0.05$ (AMs + *Ops-H. capsulatum* vs. other groups). One-way ANOVA and Tukey's multiple comparison tests were used. Data are representative of one (A–C) and two (D) independent experiments (n = 4, \pm SEM).

DISCUSSION

Histoplasmosis is a fungal disease that affects the lungs, especially in immunocompromised patients worldwide (1). Previously, we demonstrated that the host control of *H. capsulatum* infection was dependent on the production of cytokines and lipid mediators (8, 9). The specific importance of endogenous PGs in this lung fungal infection was highlighted by the treatment of *H. capsulatum*-infected mice with a selective inhibitor of COX-2, which primarily reduced PG synthesis while increasing LTB₄ production (presumably through shunting of AA metabolism), consequently reducing inflammation and increasing the resolution of the infection (8, 9). Nevertheless, a well-orchestrated pulmonary host response against infection requires activation of AMs, which themselves produce and respond to mediators that regulate critical functions such as phagocytosis and killing of microorganisms (7, 14, 15, 40, 41). The investigation of lipid mediator effects on AMs is extremely relevant (42, 43), since these cells contribute to innate and adaptive immune response triggered by microorganisms (5). It has been suggested that PGE₂ and PGD₂ can induce opposite, antagonistic actions (10), but nothing has been described about the effects of these two PGs on AM functions during *H. capsulatum* infection. Therefore, in the present study, we explored distinctive roles of PGE₂ and PGD₂ in AM effector functions after in vitro *Ops-H. capsulatum* infection.

Our results demonstrate that PGD₂ has a protective role, by enhancing the phagocytosis and killing of *Ops-H. capsulatum*, whereas PGE₂ contributes to susceptibility, by impairing phagocytosis and fungicidal capacity of AMs. Investigation of the receptors involved in PGD₂ actions revealed that DP2 is a key receptor in exogenous PGD₂, boosting AM phagocytosis and killing. DP2 is a receptor coupled to subunit G α i of G protein (21), which is a molecule involved in elevation of intracellular calcium and reduction of cAMP production (21). The role of cAMP in

macrophage effector mechanisms is well documented; there is a strong inverse correlation between the production of this second messenger and the ability of macrophages to engage in phagocytosis and killing (15, 44, 45). Thus, we suggest that PGD₂-induced improvements in AM phagocytosis and killing are likely the result of decreased cAMP levels via DP2 receptors (17, 21). Conversely, we demonstrated that exogenous PGD₂, signaling via DP2, increased the phagocytosis and killing of *Ops-H. capsulatum*. Treatment with DP2 antagonist, in the presence of exogenous PGD₂, may impair the control on cAMP levels and activation of PKA, resulting in the inhibition of effector mechanisms of macrophages and other cells (18–20). Furthermore, we investigated the action of DP1 or DP2 antagonists on endogenous PGD₂ produced by infected AMs, and we did not observe any effects on phagocytosis and killing activity. Therefore, we suggest that DP1 and DP2 are differentially expressed in AMs, resulting in distinct and opposite cell signaling, as previously described (18, 42).

As opposed to PGD₂, we found that PGE₂ inhibited effector AM mechanisms, and its actions were mediated by both EP2 and EP4 receptors. Engagement of PGE₂ on EP2 and EP4 inhibits Fc γ R-mediated phagocytosis and bacterial killing, by mechanisms driven by elevation of cAMP (14, 15). Also, we investigated the action of EP2 or EP4 antagonists alone on endogenous PGE₂ produced by infected AMs and reduced on phagocytosis and fungicidal activity were observed. We speculated that blocking only one of these receptors might have resulted in compensatory increases in the endogenous signaling of the other receptor pathway. The involvement of cAMP as a key element in the actions of PGE₂ and PGD₂ on AM effector function is also supported by the impact of these two lipids on cytokine production (20, 42, 46). Other work demonstrated that cAMP upregulates IL-10 and inhibits TNF- α synthesis (47). Also, increased release of cAMP prevented the generation of reactive oxygen and nitrogen intermediates, phagosome

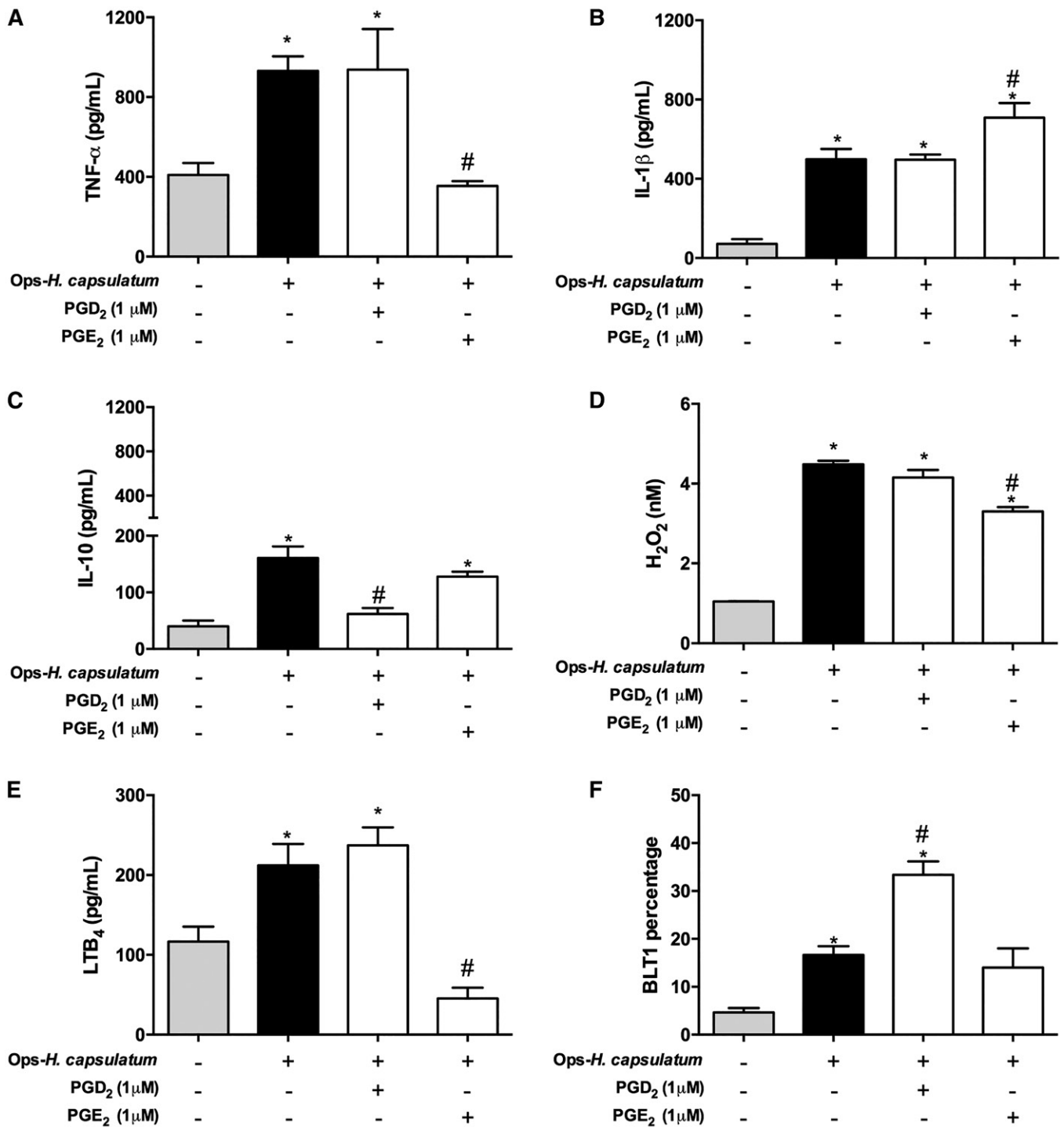


Fig. 6. TNF- α , IL-1 β , IL-10, H₂O₂, and LTB₄ production and BLT1 receptor expression by infected AMs induced by exogenous PGD₂ and PGE₂. AMs were pretreated with PGD₂ (1 μ M) or with PGE₂ (1 μ M) for 2 min before infection with *Ops-H. capsulatum* (MOI 1:10). The supernatants were collected after 48 h of incubation and TNF- α (A), IL-1 β (B), IL-10 (C), H₂O₂ (D), and LTB₄ (E) concentrations were determined by immunoassays. F: Expression of BLT1 receptor shown was analyzed by flow cytometry. * $P < 0.05$ (uninfected AMs vs. other groups); # $P < 0.05$ (AMs + *Ops-H. capsulatum* vs. other groups). One-way ANOVA and Tukey's multiple comparison tests were used. Data are representative of two independent experiments (\pm SEM).

acidification and lysosomal enzyme release, and consequently microorganism killing (48). In histoplasmosis, effective host defense requires the production of cytokines, such IL-12, IFN- γ , TNF- α , IL-1 β (20, 36, 37, 39), and LTB₄ (9), which, acting via BLT1 receptors, contribute to the elimination of the fungus (49). In contrast, IL-10 is a

negative regulator that inhibits phagosome maturation, leading to profound intracellular proliferation of microorganisms (50). Production of these cytokines is under the control of the transcription factor NF- κ B, which translocates to the nucleus after activation of MAPK pathway in response to pathogens (51). Infection of AMs with

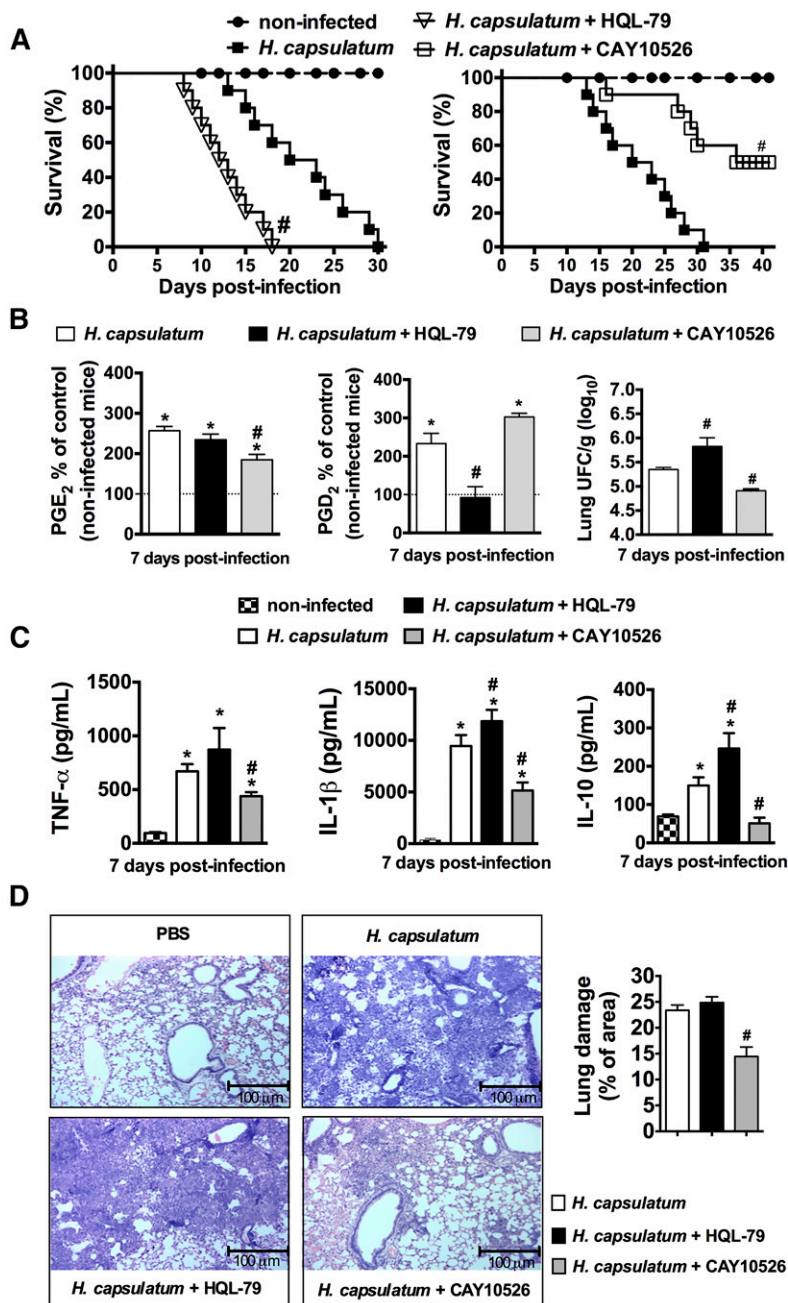



Fig. 7. PG synthesis inhibition differently affects the survival of mice infected with lethal inoculum of *H. capsulatum* and inflammatory parameters. **A:** Mice were treated daily orally with water or HQL-79 (inhibitor of PGD₂ synthesis: 3 mg/kg/0.5 ml) for 30 days (n = 10) or treated daily with CAY10526 (inhibitor of PGE₂ synthesis: 5 mg/kg/0.5 ml) for 40 days (n = 10). A group of noninfected mice was used as controls (n = 10). **B:** Lipid mediators PGD₂ and PGE₂ in the lung parenchyma were measured by enzyme immunoassay and fungal burden in the lungs. **C:** Lung cytokine concentrations (TNF-α, IL-1β, and IL-10) were determined at 7 days following infection by ELISA. **D:** Lung tissues were also processed and stained with H&E to detect leukocyte infiltration after 7 days. Percent of cell infiltrated area corresponding to extent of lung damage. # *P* < 0.05 (*H. capsulatum* + H₂O vs. *H. capsulatum* + HQL-79 or *H. capsulatum* + CAY10526 treatment); * *P* < 0.05 [PBS (non-infected mice, dashed line) vs. *H. capsulatum* + H₂O or *H. capsulatum* + HQL-79 or *H. capsulatum* + CAY10526 treatment]. **A:** Log rank test for survival analysis was used. **B–D:** One-way ANOVA and Tukey's multiple comparison test were used. Data are representative of two independent experiments (±SEM).

Ops-*H. capsulatum* induced phosphorylation of p38 MAPK, JNK1/2, and PLC-γ. Interestingly, PGE₂ treatment in AMs within 30 min of infection increased the phosphorylation of JNK1/2, with subsequent inhibition of phosphorylation of p38 after 120 min of infection and reduced NF-κB/AP-1 activity and TNF-α production after 24 h. In this regard, it was previously demonstrated that p38 signaling is important for TNF-α production and macrophage activation (52), whereas PKA activation is necessary for downregulation of TNF-α by lipopolysaccharide (53). Activation of JNK can be negatively regulated by NF-κB (54). Based on these findings, we hypothesized that activation of the MAPK, PLC-γ, and NF-κB/AP-1 pathways by PGE₂ and PGD₂ in Ops-*H. capsulatum*-infected AMs contributed differently to phagocytosis and fungicidal activity. Further studies are needed to investigate the pivotal role of these

pathways in AM effector functions and the cross-talk between them. Moreover, we demonstrated that PGD₂ reduced IL-10 production by AMs, and inhibition of PGD₂ production in vivo enhanced IL-10 release in the *H. capsulatum* infected lung, which correlated with increased phagocytosis and killing of *H. capsulatum*. In contrast, PGE₂ treatment inhibited the production of TNF-α and H₂O₂, which are important mediators of macrophage activation and killing (55, 56). Finally, we demonstrated the effects of PGD₂ that were opposite to those of PGE₂ during *H. capsulatum* infection in mice. While PGD₂ showed protective effects in infected mice, PGE₂ showed suppressive action in the lung during infection. On this model, inhibition of PGE₂ production diminished inflammatory cell infiltrate and lung damage, accompanied by reduced production of TNF-α and IL-1β.

To our knowledge, the present study describes, for the first time, the role of PGE₂ and PGD₂ in AM effector mechanisms in the context of *H. capsulatum* infection. We demonstrated a new role for PGD₂ as a key mediator for effective phagocytosis and fungicidal functions of AMs. On the other hand, these studies revealed that PGE₂ impairs phagocytosis and killing of the fungus. Notwithstanding, these findings shed light on novel perspectives for the treatment of fungal diseases using PGD₂ as a potential pharmacological immunomodulatory agent to control the infection. 

We would like to thank Dr. Huy Ong at the University of Montréal (Canada) for kindly donating the RAW-Blue™ cells used in this study; Elaine Floreano Peixoto for helping with the histology techniques; and Fabiana Rosseto de Moraes for helping with Flow Cytometer analysis.

REFERENCES

- Kauffman, C. A. 2009. Histoplasmosis. *Clin. Chest Med.* **30**: 217–225.
- Kasuga, T., T. J. White, G. Koenig, J. McEwen, A. Restrepo, E. Castaneda, C. Lacaz, E. M. Heins-Vaccari, R. S. De Freitas, R. M. Zancope-Oliveira, et al. 2003. Phylogeography of the fungal pathogen *Histoplasma capsulatum*. *Mol. Ecol.* **12**: 3383–3401.
- Colombo, A. L., A. Tobon, A. Restrepo, F. Queiroz-Telles, and M. Nucci. 2011. Epidemiology of endemic systemic fungal infections in Latin America. *Med. Mycol.* **49**: 785–798.
- Antinori, S. 2014. *Histoplasma capsulatum*: more widespread than previously thought. *Am. J. Trop. Med. Hyg.* **90**: 982–983.
- Lohmann-Matthes, M. L., C. Steinmuller, and G. Franke-Ullmann. 1994. Pulmonary macrophages. *Eur. Respir. J.* **7**: 1678–1689.
- Medeiros, A. I., A. Sá-Nunes, W. M. Turato, A. Secatto, F. G. Frantz, C. A. Sorgi, C. H. Serezani, G. S. Deepe, Jr., and L. H. Faccioli. 2008. Leukotrienes are potent adjuvant during fungal infection: effects on memory T cells. *J. Immunol.* **181**: 8544–8551.
- Secatto, A., L. C. Rodrigues, C. H. Serezani, S. G. Ramos, M. Dias-Baruffi, L. H. Faccioli, and A. I. Medeiros. 2012. 5-Lipoxygenase deficiency impairs innate and adaptive immune responses during fungal infection. *PLoS One.* **7**: e31701.
- Pereira, P. A., B. C. Trindade, A. Secatto, R. Nicolette, C. Peres-Buzalaf, S. G. Ramos, R. Sadikot, S. Bitencourt Cda, and L. H. Faccioli. 2013. Celecoxib improves host defense through prostaglandin inhibition during *Histoplasma capsulatum* infection. *Mediators Inflamm.* **2013**: 950981.
- Medeiros, A. I., A. Sa-Nunes, E. G. Soares, C. M. Peres, C. L. Silva, and L. H. Faccioli. 2004. Blockade of endogenous leukotrienes exacerbates pulmonary histoplasmosis. *Infect. Immun.* **72**: 1637–1644.
- Harris, S. G., J. Padilla, L. Koumas, D. Ray, and R. P. Phipps. 2002. Prostaglandins as modulators of immunity. *Trends Immunol.* **23**: 144–150.
- Joo, M., and R. T. Sadikot. 2012. PGD synthase and PGD₂ in immune response. *Mediators Inflamm.* **2012**: 503128.
- Joo, M., M. Kwon, R. T. Sadikot, P. J. Kingsley, L. J. Marnett, T. S. Blackwell, R. S. Peebles, Y. Urade, Jr., and J. W. Christman. 2007. Induction and function of lipocalin prostaglandin D synthase in host immunity. *J. Immunol.* **179**: 2565–2575.
- Nakanishi, M., and D. W. Rosenberg. 2013. Multifaceted roles of PGE₂ in inflammation and cancer. *Semin. Immunopathol.* **35**: 123–137.
- Serezani, C. H., J. Chung, M. N. Ballinger, B. B. Moore, D. M. Aronoff, and M. Peters-Golden. 2007. Prostaglandin E₂ suppresses bacterial killing in alveolar macrophages by inhibiting NADPH oxidase. *Am. J. Respir. Cell Mol. Biol.* **37**: 562–570.
- Aronoff, D. M., C. Canetti, and M. Peters-Golden. 2004. Prostaglandin E₂ inhibits alveolar macrophage phagocytosis through an E-prostanoid 2 receptor-mediated increase in intracellular cyclic AMP. *J. Immunol.* **173**: 559–565.
- Zoccal, K. F., C. A. Sorgi, J. I. Hori, F. W. G. Paula-Silva, E. C. Arantes, C. H. Serezani, D. S. Zamboni, and L. H. Faccioli. 2016. Opposing roles of LTB₄ and PGE₂ in regulating the inflammasome-dependent scorpion venom-induced mortality. *Nat. Commun.* **7**: 10760.
- Hirai, H., K. Tanaka, O. Yoshie, K. Ogawa, K. Kenmotsu, Y. Takamori, M. Ichimasa, K. Sugamura, M. Nakamura, S. Takano, et al. 2001. Prostaglandin D₂ selectively induces chemotaxis in T helper type 2 cells, eosinophils, and basophils via seven-transmembrane receptor CRTH2. *J. Exp. Med.* **193**: 255–261.
- Jandl, K., E. Stacher, Z. Balint, E. M. Sturm, J. Maric, M. Peinhaupt, P. Luschnig, I. Aringer, A. Fauland, V. Konya, et al. 2016. Activated prostaglandin D₂ receptors on macrophages enhance neutrophil recruitment into the lung. *J. Allergy Clin. Immunol.* **137**: 833–843.
- Chen, Y., B. Perussia, and K. S. Campbell. 2007. Prostaglandin D₂ suppresses human NK cell function via signaling through D prostanoid receptor. *J. Immunol.* **179**: 2766–2773.
- Faveeuw, C., P. Gosset, F. Bureau, V. Angeli, H. Hirai, T. Maruyama, S. Narumiya, M. Capron, and F. Trottein. 2003. Prostaglandin D₂ inhibits the production of interleukin-12 in murine dendritic cells through multiple signaling pathways. *Eur. J. Immunol.* **33**: 889–898.
- Sawyer, N., E. Cauchon, A. Châteauneuf, R. P. Cruz, D. W. Nicholson, K. M. Metters, G. P. O'Neill, and F. G. Gervais. 2002. Molecular pharmacology of the human prostaglandin D₂ receptor, CRTH2. *Br. J. Pharmacol.* **137**: 1163–1172.
- Ubersax, J. A., and J. E. Ferrell, Jr. 2007. Mechanisms of specificity in protein phosphorylation. *Nat. Rev. Mol. Cell Biol.* **8**: 530–541.
- Han, J., and R. J. Ulevitch. 2005. Limiting inflammatory responses during activation of innate immunity. *Nat. Immunol.* **6**: 1198–1205.
- Mancuso, P., and M. Peters-Golden. 2000. Modulation of alveolar macrophage phagocytosis by leukotrienes is Fc receptor-mediated and protein kinase C-dependent. *Am. J. Respir. Cell Mol. Biol.* **23**: 727–733.
- Assis, P. A., M. S. Espindola, F. W. Paula-Silva, W. M. Rios, P. A. Pereira, S. C. Leao, C. L. Silva, and L. H. Faccioli. 2014. *Mycobacterium tuberculosis* expressing phospholipase C subverts PGE₂ synthesis and induces necrosis in alveolar macrophages. *BMC Microbiol.* **14**: 128.
- Wang, J. W., D. F. Woodward, J. L. Martos, C. L. Cornell, R. W. Carling, P. J. Kingsley, and L. J. Marnett. 2016. Multitargeting of selected prostanoid receptors provides agents with enhanced anti-inflammatory activity in macrophages. *FASEB J.* **30**: 394–404.
- Aritake, K., Y. Kado, T. Inoue, M. Miyano, and Y. Urade. 2006. Structural and functional characterization of HQL-79, an orally selective inhibitor of human hematopoietic prostaglandin D synthase. *J. Biol. Chem.* **281**: 15277–15286.
- Peck, R. 1985. A one-plate assay for macrophage bactericidal activity. *J. Immunol. Methods.* **82**: 131–140.
- Brummer, E., and D. A. Stevens. 1995. Antifungal mechanisms of activated murine bronchoalveolar or peritoneal macrophages for *Histoplasma capsulatum*. *Clin. Exp. Immunol.* **102**: 65–70.
- Pick, E., J. Charon, and D. Mizel. 1981. A rapid densitometric microassay for nitroblue tetrazolium reduction and application of the microassay to macrophages. *J. Reticuloendothel. Soc.* **30**: 581–593.
- Zoccal, K. F., S. Bitencourt Cda, F. W. Paula-Silva, C. A. Sorgi, K. de Castro Figueiredo Bordon, E. C. Arantes, and L. H. Faccioli. 2014. TLR2, TLR4 and CD14 recognize venom-associated molecular patterns from *Tityus serrulatus* to induce macrophage-derived inflammatory mediators. *PLoS One.* **9**: e88174.
- Matsushita, N., M. Hizue, K. Aritake, K. Hayashi, A. Takada, K. Mitsui, M. Hayashi, I. Hirotsu, Y. Kimura, T. Tani, et al. 1998. Pharmacological studies on the novel antiallergic drug HQL-79: I. Antiallergic and antiasthmatic effects in various experimental models. *Jpn. J. Pharmacol.* **78**: 1–10.
- Coulombe, F., J. Jaworska, M. Verway, F. Tzelepis, A. Massoud, J. Gillard, G. Wong, G. Kobinger, Z. Xing, C. Couture, et al. 2014. Targeted prostaglandin E₂ inhibition enhances antiviral immunity through induction of type I interferon and apoptosis in macrophages. *Immunity.* **40**: 554–568.
- Tristão, F. S., P. C. Leonello, L. A. Nagashima, A. Sano, M. A. Ono, and E. N. Itano. 2012. Carbohydrate-rich high-molecular-mass antigens are strongly recognized during experimental *Histoplasma capsulatum* infection. *Rev. Soc. Bras. Med. Trop.* **45**: 232–237.
- Schröder, R., N. Merten, J. M. Mathiesen, L. Martini, A. Kruljac-Letunic, F. Krop, A. Blaukat, Y. Fang, E. Tran, T. Ulven, et al. 2009. The C-terminal tail of CRTH2 is a key molecular determinant that constrains Galphai and downstream signaling cascade activation. *J. Biol. Chem.* **284**: 1324–1336.

36. Deepe, G. S., Jr., and R. S. Gibbons. 2006. T cells require tumor necrosis factor- α to provide protective immunity in mice infected with *Histoplasma capsulatum*. *J. Infect. Dis.* **193**: 322–330.
37. Allendoerfer, R., and G. S. Deepe, Jr. 1998. Blockade of endogenous TNF- α exacerbates primary and secondary pulmonary histoplasmosis by differential mechanisms. *J. Immunol.* **160**: 6072–6082.
38. Peng, J. K., J. S. Lin, J. T. Kung, F. D. Finkelman, and B. A. Wu-Hsieh. 2005. The combined effect of IL-4 and IL-10 suppresses the generation of, but does not change the polarity of, type-1 T cells in Histoplasma infection. *Int. Immunol.* **17**: 193–205.
39. Deepe, G. S., Jr., and M. McGuinness. 2006. Interleukin-1 and host control of pulmonary histoplasmosis. *J. Infect. Dis.* **194**: 855–864.
40. Soares, E. M., K. L. Mason, L. M. Rogers, C. H. Serezani, L. H. Faccioli, and D. M. Aronoff. 2013. Leukotriene B4 enhances innate immune defense against the puerperal sepsis agent *Streptococcus pyogenes*. *J. Immunol.* **190**: 1614–1622.
41. Serezani, C. H., S. Kane, A. I. Medeiros, A. M. Cornett, S. H. Kim, M. M. Marques, S. P. Lee, C. Lewis, E. Bourdonnay, M. N. Ballinger, et al. 2012. PTEN directly activates the actin depolymerization factor cofilin-1 during PGE2-mediated inhibition of phagocytosis of fungi. *Sci. Signal.* **5**: ra12.
42. Tajima, T., T. Murata, K. Aritake, Y. Urade, H. Hirai, M. Nakamura, H. Ozaki, and M. Hori. 2008. Lipopolysaccharide induces macrophage migration via prostaglandin D(2) and prostaglandin E(2). *J. Pharmacol. Exp. Ther.* **326**: 493–501.
43. Pereira, P. A., S. Bitencourt Cda, D. F. dos Santos, R. Nicolette, G. M. Gelfuso, and L. H. Faccioli. 2015. Prostaglandin D2-loaded microspheres effectively activate macrophage effector functions. *Eur. J. Pharm. Sci.* **78**: 132–139.
44. Rogers, L. M., T. Thelen, K. Fordyce, E. Bourdonnay, C. Lewis, H. Yu, J. Zhang, J. Xie, C. H. Serezani, M. Peters-Golden, et al. 2014. EP4 and EP2 receptor activation of protein kinase A by prostaglandin E2 impairs macrophage phagocytosis of *Clostridium sordellii*. *Am. J. Reprod. Immunol.* **71**: 34–43.
45. Peres, C. M., D. M. Aronoff, C. H. Serezani, N. Flamand, L. H. Faccioli, and M. Peters-Golden. 2007. Specific leukotriene receptors couple to distinct G proteins to effect stimulation of alveolar macrophage host defense functions. *J. Immunol.* **179**: 5454–5461.
46. Hilkens, C. M., A. Snijders, F. G. Snijdwint, E. A. Wierenga, and M. L. Kapsenberg. 1996. Modulation of T-cell cytokine secretion by accessory cell-derived products. *Eur. Respir. J. Suppl.* **22**: 90s–94s.
47. Kim, S. H., C. H. Serezani, K. Okunishi, Z. Zaslon, D. M. Aronoff, and M. Peters-Golden. 2011. Distinct protein kinase A anchoring proteins direct prostaglandin E2 modulation of Toll-like receptor signaling in alveolar macrophages. *J. Biol. Chem.* **286**: 8875–8883.
48. Serezani, C. H., M. N. Ballinger, D. M. Aronoff, and M. Peters-Golden. 2008. Cyclic AMP: master regulator of innate immune cell function. *Am. J. Respir. Cell Mol. Biol.* **39**: 127–132.
49. Secatto, A., E. M. Soares, G. A. Locachevic, P. A. Assis, F. W. Paula-Silva, C. H. Serezani, A. I. de Medeiros, and L. H. Faccioli. 2014. The leukotriene B(4)/BLT(1) axis is a key determinant in susceptibility and resistance to histoplasmosis. *PLoS One.* **9**: e85083.
50. Nguyen, T., N. Robinson, S. E. Allison, B. K. Coombes, S. Sad, and L. Krishnan. 2013. IL-10 produced by trophoblast cells inhibits phagosome maturation leading to profound intracellular proliferation of *Salmonella enterica Typhimurium*. *Placenta.* **34**: 765–774.
51. Lawrence, T. 2009. The nuclear factor NF- κ B pathway in inflammation. *Cold Spring Harb. Perspect. Biol.* **1**: a001651.
52. Kang, Y. J., J. Chen, M. Otsuka, J. Mols, S. Ren, Y. Wang, and J. Han. 2008. Macrophage deletion of p38 α partially impairs lipopolysaccharide-induced cellular activation. *J. Immunol.* **180**: 5075–5082.
53. Zhu, W., J. S. Downey, J. Gu, F. Di Padova, H. Gram, and J. Han. 2000. Regulation of TNF expression by multiple mitogen-activated protein kinase pathways. *J. Immunol.* **164**: 6349–6358.
54. Tang, G., Y. Minemoto, B. Dibling, N. H. Purcell, Z. Li, M. Karin, and A. Lin. 2001. Inhibition of JNK activation through NF- κ B target genes. *Nature.* **414**: 313–317.
55. Kunkel, S. L., M. Spengler, M. A. May, R. Spengler, J. Larrick, and D. Remick. 1988. Prostaglandin E2 regulates macrophage-derived tumor necrosis factor gene expression. *J. Biol. Chem.* **263**: 5380–5384.
56. Sporn, P. H., M. Peters-Golden, and R. H. Simon. 1988. Hydrogen-peroxide-induced arachidonic acid metabolism in the rat alveolar macrophage. *Am. Rev. Respir. Dis.* **137**: 49–56.